Earth's middle age

Peter A. Cawood[1,2]* and Chris J. Hawkesworth[1]
[1]Department of Earth Sciences, University of St Andrews, Irvine Building, North Street, St Andrews, Fife KY16 9AL, UK
[2]School of Earth and Environment, University of Western Australia, Crawley, Western Australia 6009, Australia

ABSTRACT

Earth's middle age, extending from 1.7 to 0.75 Ga, was characterized by environmental, evolutionary, and lithospheric stability that contrasts with the dramatic changes in preceding and succeeding eras. The period is marked by a paucity of preserved passive margins, an absence of a significant Sr anomaly in the paleoseawater record and in the $\varepsilon_{Hf(t)}$ in detrital zircon, a lack of orogenic gold and volcanic-hosted massive sulfide deposits, and an absence of glacial deposits and iron formations. In contrast, anorthosites and kindred bodies are well developed and major pulses of Mo and Cu mineralization, including the world's largest examples of these deposits, are features of this period. These trends are attributed to a relatively stable continental assemblage that was initiated during assembly of the Nuna supercontinent by ca. 1.7 Ga and continued until breakup of its closely related successor, Rodinia, ca. 0.75 Ga. The overall low abundance of passive margins is consistent with a stable continental configuration, which also provided a framework for environmental and evolutionary stability. A series of convergent margin accretionary orogens developed along the edge of the supercontinent. Abundant anorthosites and related rocks developed inboard of the plate margin. Their temporal distribution appears to link with the secular cooling of the mantle, at which time the overlying continental lithosphere was strong enough to be thickened and to support the emplacement of large plutons into the crust, yet the underlying mantle was still warm enough to result in widespread melting of the lower thickened crust.

INTRODUCTION

Earth's rock record is incomplete, with a heterogeneous distribution of rock units and events that correspond to periods of supercontinent assembly (Cawood et al., 2013). For example, U-Pb zircon crystallization ages (Voice et al., 2011), whether determined from igneous rocks or detrital sediments, and the age distribution of metamorphic rocks (Brown, 2007) show peaks in the frequency of occurrence at the time of supercontinent assembly (Bradley, 2011). The period 1.7–0.75 Ga, however, is anomalous (Fig. 1) in that it is characterized by the following.

1. A paucity of passive margins (Bradley, 2008), and notably no passive margin age peak corresponding with the phase of assembly of the Rodinia supercontinent as there is for the preceding Nuna and succeeding Gondwana cycles.

2. An absence of glacial deposits (Bradley, 2011) and iron formations (Bekker et al., 2010).

3. No significant Sr anomaly in the paleoseawater record (Shields, 2007) or in the $\varepsilon_{Hf(t)}$ record in detrital zircon (Belousova et al., 2010).

4. A lack of phosphate deposits, even though they were well established ca. 2.2–1.8 Ga and after 0.75 Ga (Papineau, 2010), periods that also correspond with maxima in the geological record in black shale abundance and in the chemical index of alteration (Condie et al., 2001). Such patterns suggest major global changes in ocean and atmospheric chemistry in the Paleoproterozoic and Neoproterozoic, and perhaps more stable conditions in the intervening interval (cf. Brasier and Lindsay, 1998).

5. Relatively high ocean salinity before a significant decrease after 800 Ma in association with the development of major evaporate basins, possibly linked to increased sulfate delivery and development of S-rich porphyry deposits in the Phanerozoic (Richards and Mumin, 2013).

6. Massif-type anorthosites and kindred bodies, also variously termed A-type granite, anorogenic granite, anorthosite-mangerite-charnockite-granite suite, ferroan feldspathic granitoids, ilmenite-granite, or Rapakivi granites, are characteristic features of the Proterozoic, largely in the period 1.8–1.0 Ga (Ashwal, 2010).

7. Limited orogenic gold deposits between 1.7 and 0.9 Ga, accounting for significantly less than 1% of known production, yet corresponding to the generation of almost 20% of the preserved crustal record (Goldfarb et al., 2001). Volcanic-hosted massive sulfide (VHMS) deposits show a similar distribution (Huston et al., 2010). Sedimentary rock-hosted manganese deposits are also conspicuous by their absence between 1.8 and 0.8 Ga; Maynard (2010) suggested that this corresponds to the low frequency of black shale deposition and may relate to a monotonous low-oxygen ocean, with nonsulfidic deep water. Sedimentary rock–hosted stratiform copper deposits are largely absent from the rock record between 1.8 and 0.8 Ga (Hitzman et al., 2010).

PALEOGEOGRAPHIC CONFIGURATIONS

The pattern of rock units and the events outlined in Figure 1 indicate that the period from ca. 1.7 Ga to 0.75 Ga, herein termed Earth's middle age, was unique with respect to preceding and succeeding eras of Earth history (cf. Holland, 2006). This period encompasses the proposed Rodinian supercontinent cycle (ca. 1.3–0.75 Ga) and part of the Nuna cycle (ca. 2.1–1.3 Ga). There is increasing evidence that the change from Nuna to Rodinia was one of transition in which Siberia, Laurentia, and Baltica formed a stable core that assembled during construction of Nuna by 1.8–1.7 Ga and continued, with little change in configuration, until Rodinia breakup at 0.75 Ga (e.g., Evans, 2013). This contrasts with the significant changes in continental configurations that occurred in the initial assembly of Nuna or in the transition from Rodinia breakup to Pangea assembly. Extension-related magmatism at ca. 1.4–1.25 Ga is widespread around parts of Laurentia, Baltica, and Siberia and is ascribed to Nuna breakup (Evans, 2013). However, the general paucity of passive margins through the Mesoproterozoic (Fig. 1) and the absence of any evidence for 1.1–1.0 Ga orogenesis in blocks such as Siberia (Gladkochub et al., 2010) argue for no significant breakup and reassembly of these continental fragments in the transition from Nuna to Rodinia (cf. Bradley, 2008).

The overall stability in the configuration of the core components of Nuna and Rodinia is mimicked in the presence of a long-lived accretionary orogen that developed along the margins of Laurentia, Baltica, Australia, and Amazonia from ca. 1.8 Ga to 1.25 Ga (e.g., Whitmeyer and Karlstrom, 2007). Accretionary activity terminated with the 1.25–0.95 Ga Grenville orogeny and equivalent tectonothermal events leading to final assembly of Rodinia, which involved collision assembly of Amazonia, India, and related fragments onto the stable Nuna core. These events resulted in the 1.1–1.0 Ga peak in granulite and eclogite facies metamorphism (Fig. 1; Brown, 2007).

IMPLICATIONS

Rock units and events depicted in Figure 1 span surficial (atmosphere, oceans, biosphere) and deep Earth (lithospheric) proxies, and their temporal equivalence suggests that they are linked and therefore controlled through common processes. Drivers that tie across different aspects of the Earth system and exert long-term control on the rock record include (1) tectonic processes associated with the structure, interactions, and configurations of the lithosphere, and (2) the secular evolution of

*E-mail: peter.cawood@st-andrews.ac.uk.

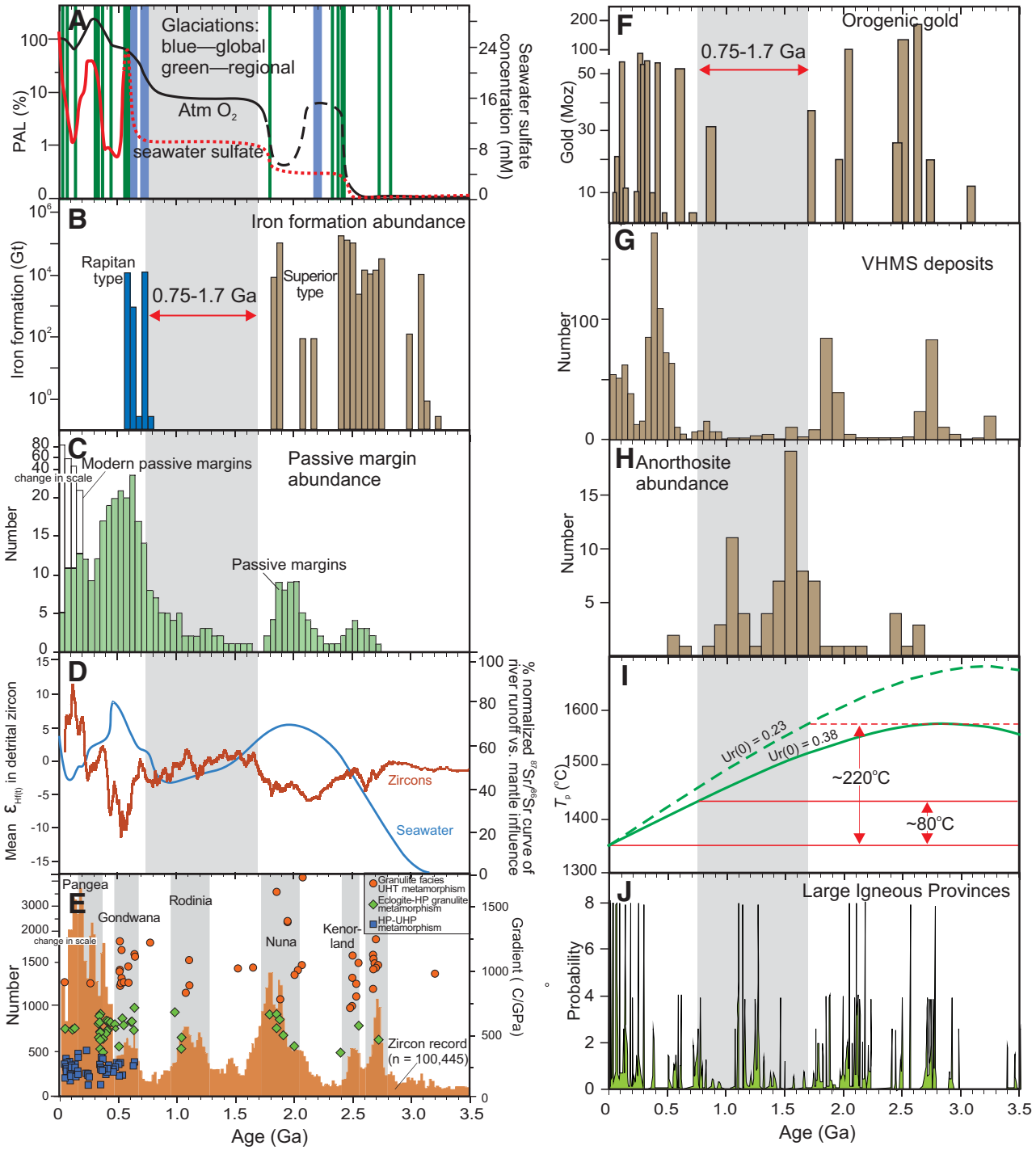

Figure 1. A: Temporal distribution of glaciations (Bradley, 2011), atmospheric (Atm) oxygen relative to present atmospheric level (PAL) (Berner et al., 2003; Canfield, 2005), and seawater sulfate (adapted from Farquhar et al., 2010; Pope and Grotzinger, 2003). B: Iron formation abundance (Bekker et al., 2010). C: Ages of ancient and modern passive margins (Bradley, 2008). D: Normalized seawater $^{87}Sr/^{86}Sr$ curve (Shields, 2007) and running mean of initial ε_{Hf} in ~7000 detrital zircons from recent sediments (Cawood et al., 2013). E: Histogram of more than 100,000 detrital zircon analyses showing several peaks in their U-Pb crystallization ages over course of Earth history (Voice et al., 2011) that are very similar to ages of supercontinent assembly (timing of assembly shown). Also shown is apparent thermal gradient versus age of peak metamorphism for three main types of granulite facies metamorphic belts (Brown, 2007). UHT—ultrahigh temperature; HP—high pressure; UHP—ultrahigh pressure. F: Orogenic gold (adapted from Goldfarb et al., 2001). G: Volcanic-hosted massive sulfide (VHMS) deposits (Mosier et al., 2009). H: Anorthosite abundance (compiled from Ashwal, 2010; Frost and Frost, 2013; Parnell et al., 2012). I: Thermal (*T*, temperature) models for ambient mantle for Urey (Ur) ratios of 0.23 and 0.38 (Herzberg et al., 2010). J: Time series analysis of distribution of large igneous provinces (Prokoph et al., 2004). Period 1.7–0.75 Ga is highlighted.

Earth's internal heat production. The absence of any change in the inferred frequency of large igneous provinces across the 1.7–0.75 Ga time period (Fig. 1), relative to preceding and succeeding intervals, suggests that processes within the deep mantle were not a significant factor.

Unusually, the configuration of core elements of the Nuna supercontinent over the period ca. 2.1–1.7 Ga continued until ca. 0.8 Ga, when the inferred succeeding supercontinent of Rodinia started to break up (Evans, 2013). Paleogeographic reconstructions suggest that the supercontinent assemblage straddled equatorial and temporal climatic zones throughout the intervening time frame; there is little or no evidence for continental fragments in polar latitudes (Evans, 2013, and references therein). A consequence of a limited breakup history is a paucity of passive margins in the range 1.8–0.8 Ga (Fig. 1; Bradley, 2008). This stable configuration in both space and time provides the primary constraint on the environmental stasis that characterizes the oceans, atmosphere, and biosphere (Brasier and Lindsay, 1998). In detail, the ocean was relatively warm and sulfidic euxinic (Farquhar et al., 2010), as evidenced by the absence of glacial deposits and iron formations. The subdued seawater Sr and zircon Hf isotopic signatures from 1.7 to 0.75 Ga likely reflect the long accretionary history and juvenile magmatism, combined with inferred ocean closure through dual subduction zones beneath the opposing Laurentian and Amazonian margins (Cawood et al., 2013; Spencer et al., 2013). The general trend of seawater Sr values is in part mimicked by seawater sulfate (Fig. 1). Pope and Grotzinger (2003) linked the ca. 1.7 Ga change from halite to gypsum as the main evaporite phase to increasing seawater sulfate values along with decreasing oversaturation in seawater of calcium carbonate. Increasing input to seawater of sulfate around that time corresponds with Nuna assembly, suggesting that the source of the sulfate runoff was from chemical weathering of the continental crust in response to collisional orogenesis and growth of major mountain chains. The change in seawater proxies in the late Neoproterozoic corresponds with the introduction of high-pressure metamorphic assemblages into the rock record and a pulse of crustal reworking associated with Gondwana assembly, as evidenced by $\varepsilon_{Hf(t)}$ values in detrital zircons. These features may reflect an increasing scale of collision-generated mountain ranges, which in turn links to increases in weathering, erosion, and runoff, as reflected in seawater composition.

The anorthosites and related igneous activity during Earth's middle age are spatially and temporally linked to convergent plate margins and occur in either synsubduction or postcollisional settings (McLelland et al., 2010; Whitmeyer and Karlstrom, 2007). Phase equilibria and geochemistry for these plutons suggest that the enhanced upper mantle thermal conditions resulted in extensive melting of a thickened arc root with variable input of a mantle component at 10–13 kbar (40–50 km) at ~950–1000 °C (Bédard, 2009). The spatial constraint of a convergent plate margin setting does not, however, account for the temporal preponderance of these pluton types to the period 1.8–1.0 Ga (Fig. 1). Rather, it is linked to secular cooling of the mantle to a temperature at which the overlying continental lithosphere was strong enough to be both thickened and to support the emplacement of large plutons into the crust, yet still warm enough to result in widespread melting of the lower thickened crust.

Since 3 Ga the upper mantle has progressively cooled, and it may have been at temperatures 220 °C and 80 °C hotter than today at 1.7 Ga and 0.75 Ga, respectively (Herzberg et al., 2010). Geodynamic modeling studies indicate that mantle temperature is a prime control on lithosphere behavior, influencing the processes by which the plates interact. Sizova et al. (2010) highlighted that at mantle temperatures above ΔT = 250 °C (relative to present-day values), there is no subduction, the lithosphere is weak and deforms internally, and continental plates are fragmented by spreading centers. Between ΔT = 250 and 160 °C, plates are still weak and deform internally due to melt percolation, but oceanic plates can underthrust continental plates along shallow subduction zones. Plate interaction of the type observed on Earth today requires mantle temperatures below ΔT = 160 °C. In collision zones, mantle temperatures hotter than ΔT = 80 °C appear to preclude deep subduction of the continental crust due to shallow depth of breakoff of the attached subducting oceanic lithosphere, resulting in an absence of ultrahigh-pressure metamorphism (Sizova et al., 2014). The restriction of ultrahigh-pressure metamorphic assemblages (Fig. 1), together with the general distribution of ophiolites and the subduction- and collision-related gemstones of jadeite and ruby to the Neoproterozoic or younger, has led to the suggestion that modern plate tectonics began in the Neoproterozoic (Stern et al., 2013, and references therein).

The paucity of orogenic gold and VHMS deposits is difficult to explain based on models involving uniformitarian accretionary orogen settings (Goldfarb et al., 2001). The well-developed convergent plate boundary along the margin of Laurentia and Baltica constitutes an ideal fertile upper mantle source region for these deposit types (Hronsky et al., 2012). Secular changes in the distribution of these deposit types may reflect the changing processes of lithospheric interaction associated with decreasing mantle temperatures. Neoproterozoic and younger deposits are controlled by modern-style orogenic processes. Pre–1.7 Ga deposits reflect shallow subduction with the weak lithosphere disrupted by shear zones that acted as conduits for gold-bearing fluids. Although orogenic gold deposits were poorly developed in Earth's middle age, significant gold accumulations are present in the form of iron oxide copper-gold (IOCG) deposits (Richards and Mumin, 2013). IOCG and molybdenite mineralization, including the largest examples of these deposits (Parnell et al., 2012), are temporally linked to anorthosites and kindred intrusions and form in extensional environments in suprasubduction and postcollision settings. Richards and Mumin (2013) suggested that IOCG deposits are the Precambrian equivalent of Phanerozoic porphyry-type deposits, with the change in mineralization type related to increasing seawater sulfate in subducted oceanic lithosphere in the mid-Neoproterozoic, as well as to decreasing lithospheric geothermal gradients, resulting in a change from S-poor to S-rich arc magmas.

The termination of Earth's middle age corresponds with Rodinia breakup at 0.75 Ga. Falling mantle temperatures enabled deeper levels of slab breakoff in collision zones, and the resultant greater depths to which continental crust was subducted prior to exhumation allowed the development of high-pressure metamorphic assemblages. Elements of the rock record that showed little change during Earth's middle age show a strongly episodic distribution linked to the supercontinent cycles of Gondwana and Pangea (Fig. 1). The oxygen levels in both the atmosphere and deep oceans increased, and phosphate and evaporate deposits became widespread and provided a major spurt for metazoans evolution. The impact of changing lithospheric behavior on surficial processes is likely an ongoing event in Earth history.

ACKNOWLEDGMENTS

We thank the Natural Environment Research Council (grant NE/J021822/1) and the University of St Andrews for funding. Comments from Brendan Murphy, Sergei Pisarevsky, Tony Prave, Aubrey Zerkle and journal reviewers Dwight Bradley, Mike Brown, and Steve Whitmeyer helped clarify our ideas.

REFERENCES CITED

Ashwal, L.D., 2010, The temporality of anorthosites: Canadian Mineralogist, v. 48, p. 711–728, doi:10.3749/canmin.48.4.711.

Bédard, J. H., 2009, Parental magmas of Grenville Province massif-type anorthosites, and conjectures about why massif anorthosites are restricted to the Proterozoic, *in* Clemens, J.D., ed., Sixth Hutton Symposium on The Origin of Granites and Related Rocks: Royal Society of Edinburgh Transactions, Earth and Environmental Science, v. 100, parts 1 and 2, p. 77–103, doi.org/10.1017/S1755691009016016.

Bekker, A., Slack, J.F., Planavsky, N., Krapež, B., Hofmann, A., Konhauser, K.O., and Rouxel, O.J., 2010, Iron formation: The sedimentary product of a complex interplay among mantle, tectonic, oceanic, and biospheric process: Economic Geology and the Bulletin of the Society of Economic Geologists, v. 105, p. 467–508, doi:10.2113/gsecongeo.105.3.467.

Belousova, E.A., Kostitsyn, Y.A., Griffin, W.L., Begg, G.C., O'Reilly, S.Y., and Pearson, N.J., 2010, The growth of the continental crust: Constraints

from zircon Hf-isotope data: Lithos, v. 119, p. 457–466, doi:10.1016/j.lithos.2010.07.024.
Berner, R.A., Beerling, D.J., Dudley, R., Robinson, J.M., and Wildman, R.A., 2003, Phanerozoic atmosphere oxygen: Annual Review of Earth and Planetary Sciences, v. 31, p. 105–134, doi:10.1146/annurev.earth.31.100901.141329.
Bradley, D.C., 2008, Passive margins through Earth history: Earth-Science Reviews, v. 91, p. 1–26, doi:10.1016/j.earscirev.2008.08.001.
Bradley, D.C., 2011, Secular trends in the geologic record and the supercontinent cycle: Earth-Science Reviews, v. 108, p. 16–33, doi:10.1016/j.earscirev.2011.05.003.
Brasier, M.D., and Lindsay, J.F., 1998, A billion years of environmental stability and the emergence of eukaryotes: New data from northern Australia: Geology, v. 26, p. 555–558, doi:10.1130/0091-7613(1998)026<0555:ABYOES>2.3.CO;2.
Brown, M., 2007, Metamorphic conditions in orogenic belts: A record of secular change: International Geology Review, v. 49, p. 193–234, doi:10.2747/0020-6814.49.3.193.
Canfield, D.E., 2005, The early history of atmospheric oxygen: Homage to Robert M. Garrels: Annual Review of Earth and Planetary Sciences, v. 33, p. 1–36, doi:10.1146/annurev.earth.33.092203.122711.
Cawood, P.A., Hawkesworth, C.J., and Dhuime, B., 2013, The continental record and the generation of continental crust: Geological Society of America Bulletin, v. 125, no. 1–2, p. 14–32, doi:10.1130/B30722.1.
Condie, K.C., Des Marais, D.J., and Abbott, D., 2001, Precambrian superplumes and supercontinents: A record in black shales, carbon isotopes, and paleoclimates?: Precambrian Research, v. 106, p. 239–260, doi:10.1016/S0301-9268(00)00097-8.
Evans, D.A.D., 2013, Reconstructing pre-Pangean supercontinents: Geological Society of America Bulletin, v. 125, p. 1735–1751, doi:10.1130/B30950.1.
Farquhar, J., Wu, N., Canfield, D.E., and Oduro, H., 2010, Connections between sulfur cycle evolution, sulfur isotopes, sediments, and base metal sulfide deposits: Economic Geology and the Bulletin of the Society of Economic Geologists, v. 105, p. 509–533, doi:10.2113/gsecongeo.105.3.509.
Frost, C.D., and Frost, B.R., 2013, Proterozoic ferroan feldspathic magmatism: Precambrian Research, v. 228, p. 151–163, doi:10.1016/j.precamres.2013.01.016.
Gladkochub, D.P., Donskaya, T.V., Wingate, M.T.D., Mazukabzov, A.M., Pisarevsky, S.A., Sklyarov, E.V., and Stanevich, A.M., 2010, A one-billion-year gap in the Precambrian history of the southern Siberian Craton and the problem of the Transproterozoic supercontinent: American Journal of Science, v. 310, p. 812–825, doi:10.2475/09.2010.03.
Goldfarb, R.J., Groves, D.I., and Gardoll, S., 2001, Orogenic gold and geologic time: A global synthesis: Ore Geology Reviews, v. 18, p. 1–75, doi:10.1016/S0169-1368(01)00016-6.
Herzberg, C., Condie, K., and Korenaga, J., 2010, Thermal history of the Earth and its petrological expression: Earth and Planetary Science Letters, v. 292, p. 79–88, doi:10.1016/j.epsl.2010.01.022.
Hitzman, M.W., Selley, D., and Bull, S., 2010, Formation of sedimentary rock-hosted stratiform copper deposits through Earth history: Economic Geology and the Bulletin of the Society of Economic Geologists, v. 105, p. 627–639, doi:10.2113/gsecongeo.105.3.627.
Holland, H.D., 2006, The oxygenation of the atmosphere and oceans: Royal Society of London Philosophical Transactions, ser. B, v. 361, no. 1470, p. 903–915, doi:10.1098/rstb.2006.1838.
Hronsky, J.M.A., Groves, D.I., Loucks, R.R., and Begg, G.C., 2012, A unified model for gold mineralisation in accretionary orogens and implications for regional-scale exploration targeting methods: Mineralium Deposita, v. 47, p. 339–358, doi:10.1007/s00126-012-0402-y.
Huston, D.L., Pehrsson, S., Eglington, B.M., and Zaw, K., 2010, The geology and metallogeny of volcanic-hosted massive sulfide deposits: Variations through geologic time and with tectonic setting: Economic Geology and the Bulletin of the Society of Economic Geologists, v. 105, p. 571–591, doi:10.2113/gsecongeo.105.3.571.
Maynard, J.B., 2010, The chemistry of manganese ores through time: A signal of increasing diversity of Earth-surface environments: Economic Geology and the Bulletin of the Society of Economic Geologists, v. 105, p. 535–552, doi:10.2113/gsecongeo.105.3.535.
McLelland, J.M., Selleck, B.W., Hamilton, M.A., and Bickford, M.E., 2010, Late- to post-tectonic setting of some major Proterozoic anorthosite-mangerite-charnockite-granite (AMCG) suites: Canadian Mineralogist, v. 48, p. 729–750, doi:10.3749/canmin.48.4.729.
Mosier, D.L., Berger, V.I., and Singer, D.A., 2009, Volcanogenic massive sulfide deposits of the world—Database and grade and tonnage models: U.S. Geological Survey Open-File Report 2009–1034, 46 p.
Papineau, D., 2010, Global biogeochemical changes at both ends of the Proterozoic: Insights from phosphorites: Astrobiology, v. 10, p. 165–181, doi:10.1089/ast.2009.0360.
Parnell, J., Hole, M., Boyce, A.J., Spinks, S., and Bowden, S., 2012, Heavy metal, sex and granites: Crustal differentiation and bioavailability in the mid-Proterozoic: Geology, v. 40, p. 751–754, doi:10.1130/G33116.1.
Pope, M.C., and Grotzinger, J.P., 2003, Paleoproterozoic Stark Formation, Athapuscow Basin, northwest Canada: Record of cratonic-scale salinity crisis: Journal of Sedimentary Research, v. 73, p. 280–295, doi:10.1306/091302730280.
Prokoph, A., Ernst, R.E., and Buchan, K.L., 2004, Time-series analysis of large igneous provinces: 3500 Ma to present: Journal of Geology, v. 112, p. 1–22, doi:10.1086/379689.
Richards, J.P., and Mumin, A.H., 2013, Magmatic-hydrothermal processes within an evolving Earth: Iron oxide–copper–gold and porphyry Cu ± Mo ± Au deposits: Geology, v. 41, p. 767–770, doi:10.1130/G34275.1.
Shields, G.A., 2007, A normalised seawater strontium isotope curve: Possible implications for Neoproterozoic–Cambrian weathering rates and the further oxygenation of the Earth: eEarth, v. 2, p. 35–42, doi:10.5194/ee-2-35-2007.
Sizova, E., Gerya, T., Brown, M., and Perchuk, L.L., 2010, Subduction styles in the Precambrian: Insight from numerical experiments: Lithos, v. 116, p. 209–229, doi:10.1016/j.lithos.2009.05.028.
Sizova, E., Gerya, T., and Brown, M., 2014, Contrasting styles of Phanerozoic and Precambrian continental collision: Gondwana Research, v. 25, p. 522–545, doi:10.1016/j.gr.2012.12.011.
Spencer, C.J., Hawkesworth, C., Cawood, P.A., and Dhuime, B., 2013, Not all supercontinents are created equal: Gondwana-Rodinia case study: Geology, v. 41, p. 795–798, doi:10.1130/G34520.1.
Stern, R.J., Tsujimori, T., Harlow, G., and Groat, L.A., 2013, Plate tectonic gemstones: Geology, v. 41, p. 723–726, doi:10.1130/G34204.1.
Voice, P.J., Kowalewski, M., and Eriksson, K.A., 2011, Quantifying the timing and rate of crustal evolution: Global compilation of radiometrically dated detrital zircon grains: Journal of Geology, v. 119, p. 109–126, doi:10.1086/658295.
Whitmeyer, S.J., and Karlstrom, K.E., 2007, Tectonic model for the Proterozoic growth of North America: Geosphere, v. 3, p. 220–259, doi:10.1130/GES00055.1.

Manuscript received 19 December 2013
Revised manuscript received 5 March 2014
Manuscript accepted 6 March 2014

Printed in USA